Volume 65, Issue 1, 2021
Journal of Scientific Research
Institute of Science,
Banaras Hindu University, Varanasi, India.

Phytonutrient Assisted Synthesis and Stabilization of Silver Nanoparticles from the Leaf Extract of *Persicaria hydropiper* (L.) Delarbre and their Antibacterial Activity Studies

M. P. Somashekarappa*

Department of PG Studies in Chemistry, IDSG Government College, Chikkamagaluru, Affiliated to Kuvempu University, Karnataka State, India – 577102. psshekar1@rediffmail.com*

Abstract: **Silver nanoparticles (AgNPs) were synthesized and stabilized using the aqueous extract of *Persicaria hydroppiper* leaves. The particles were characterized using Uv-visible extinction spectroscopy, scanning electron microscopy (SEM), transmission electron microscopy (TEM) and powder X-ray diffraction (PXRD) studies. Increase in phytonutrient concentration decreases the particle size to a small extent and an increase in silver nitrate concentration increases the particle size. The average size of the AgNPs worked out using TEM and PXRD data were found to be 24-32 nm. Phytonutrient assisted reduction crystallizes the nanosized silver in to face centred cubic structure. Growth inhibition effect of the nanoparticles against *Escherichia coli (E. coli)* and *Staphylococcus aureus (S. aureus)* were determined and compared with reference antibacterial substance ciprofloxacin. The AgNPs inhibit the growth of *E. coli* and *S. aurous* bacteria to different extents with their zones of inhibition 13.0 mm and 12.0 mm respectively.**

Key words: Antibacterial activity, *Escherichia coli, Persicaria hydropiper*, Silver nanoparticls, *Staphylococcus aureus.*

I. INTRODUCTION

Special and size dependant physico-chemical properties of the nanomaterials made them useful in thousands of industrial applications (Stark et al., 2015). Fabrication of the nanomaterials in to devices and the properties possessed by the devices depends on the size shape structure and functionalization, and hence the consequent stability of the particles.

Silver nanoparticles (AgNPs) are one of the highly explored nanomaterials owing to their special properties attributable mainly to their size, shape and structure dependent surface plasmon resonance (Amendola et al., 2010). The application potential of the silver nanoparticles encompasses photocatalysis (Awazu et al., 2008), optical sensors (McFarland & Van Duyene, 2008), nanosphere lithography (Jensen et al. 2000), optoelectronics (Ko et al., 2013), solar energy conversion devices (Morfa & Rowlen, 2008) and as surface-enhanced Raman scattering (SERS) substrates (Li et al., 2010). In addition, as the AgNPs exhibit remarkable variety of antimicrobial activities (Rai et al., 2009), their biomedicinal applications are being evaluated and reviewed (Wong & Liu 2010; Prabhu & Poulose, 2012; Burdusel et al., 2018). The best manifestation of the exploration of the antimicrobial properties of the AgNPs are materials for antibacterial water filter (Jain & Pradeep 2005), activated carbon based antibacterial air filter (Yoon et al., 2008) and AgNP embedded textile fabrics with antibacterial activity (Ravindra et at., 2020; Song et al., 2012; Wu et al., 2016; Zhang et al., 2016).

Wet chemical reduction methods for the synthesis of AgNPs involve use of various stabilizing agents (Garcia-Barrasa et al., 2011), certain polymers, and cationic polynorbornenes (Baruah et al., 2013), showing that the resulting particles are unstable without any capping by molecules. Since, the reducing agents like $NaBH_4$, $LiAlH_4$, $R_4N^+(Et_3BH^-)$ or hydrazine (Schmid & Chi, 1998), used for synthesis of AgNPs contaminates the solutions with reaction byproducts such as borides, metal borates (Glavee et al., 1992) B_2H_6, $NaNO_3$ etc., the study of bacterial

* Corresponding Author

growth inhibition effects becomes complex. Stabilizing AgNPs using molecular capping makes the process expensive. The synthesis by reduction reaction and the stabilization should be done in two separate steps. Though, AgNPs synthesis by using mixed-valence polyoxometallates, polysaccharide, Tollens irradiation, and biological methods have been regarded as greener approaches (Sharma et al., 2008), using aqueous extracts of plants is one of the better, greener and cheaper methods, standing alone in recent years (Mittal et al., 2013; Rajeshkumar & Bharath, 2017). It has been proved that the AgNPs synthesized using plant extracts show relatively better sensitivity for biosensing of mancozeb fungicide and better photocatalytic property (Alex et al., 2020).

Literature survey reveals that phytonutrient assisted synthesis of AgNPs using *Persicaria hydropiper* (L.) Delarbre is not been attempted. *P. hydropiper* is a medicinal plant with tremendous medicinal properties and proved to have enormous number of medicinal applications (Moyeenul Huq et al., 2014; Ayaz et al 2020). Therefore, synthesis of AgNPs using the aqueous extract of *P. hydropiper*, an efficient and eco- friendly method was undertaken. The selected plant specimen was submitted to, and identified at Mahatma Gandhi Botanical Garden, University of Agricultural Sciences, Bengaluru, India (accession number UASB-5238). The present study involves preparation of aqueous extract of the selected plant, phytochemical analysis of the extract, synthesis of AgNPs, characterization of the particles by Uv-visible extinction spectroscopy, powder X-ray diffraction, SEM and TEM analysis, and the study of their antibacterial activities against *E. coli* and *S. aureus* bacteria.

II. RESULTS AND DISCUSSION

Concentration of the extracts prepared for the AgNP synthesis were from 5×10^{-5} g/mL to 25×10^{-5} g/mL. Extract prepared for the qualitative phytochemical analysis was approximately five to six times highly concentrated compared to that prepared for synthesis of AgNPs, since very dilute solutions did not answer the presence of phytonutrients appropriately. Results of the qualitative phytochemical analyses (Raaman, 2006) are presented in Table I.

Detailed qualitative phytochemical analysis of the extract revealed the presence of phenolic compounds and flavonoids and the results are consistent with earlier reports (Moyeenul Huq et al., 2014).

To be able to applicable in biology and medicine, AgNPs should be biocompatible in low concentration and stable in all sizes (Sharma et al., 2008). However, synthesis of AgNPs using reducing agents like sodium borohydride and without stabilizing agents results in unstable nanoparticle solutions.

Table I. Results of qualitative phytochemical analysis of the extract of *P. hydropiper*.

Phytochemicals	Test	Inference
Alkaloids	Mayer's test	−
	Wagners test	−
Carbohydrates and glycosides	Molish test	−
	Fehling's test	−
	Borntragers's test	−
Saponines	Foam test	−
Proteins and amino acids	Millon's test	−
	Biuret's test	−
	Ninhydrin test	−
Phytosteroids	Libeirman-Burchard test	−
Oils and fats	Spot test	−
	Saponification test	−
Phenolic compounds and flavonoids	Ferric chloride test	+
	Lead acetate test	+
	Alkaline test	+
	Gelatin test	−
Gum and mucilages	o-Toluidine test	−

In the current work, stable AgNP solutions were synthesized using aqueous extracts of *P. hydropiper*, without using any reducing agents, or stabilizing agents. The preparation of AgNPs by this method is fairly reproducible. The reduction of $AgNO_3$ in to metallic silver is been carried out by the phytonutrients present in the plant extract. Leaves of the *P. hydropiper* were investigated to contain thirty-two different flavonoids and fourteen different bioactive phenolic acids and sesquiterpenoids, and the literature reports were reviewed (Moyeenul Huq et al., 2014). The Ag^+ in the $AgNO_3$ undergoes reduction to Ag^0 in the form of nanoparticles assisted by the phytonutrients present in the extract as reducing agents (Rajeshkumar & Bharath, 2017; Mandal et al., 2016; Priya et al., 2016; Gopinath et al., 2016). As all the Ag^0 condenses to nanoparticle, a surface coating of the particles by the bioactive organic molecules present in the system occurs (Alex et al., 2020; Garcia, 2011). The surface coating results in the formation of a monomolecular layer on the silver surface. All the particles possess same peripheral properties and hence repel from each other in their solution. Thus, the AgNPs synthesized by this method are stable.

A. Characterization

A surface Plasmon resonance absorption band due to surface electrons on the metallic silver, in the visible region of electromagnetic radiation is a characteristic signature of the AgNPs (Taleb et al., 1998; Nogin ov et al., 2006). Formation of the AgNPs, upon addition of $AgNO_3$ solution in to extract can be visually identified by a colour change of the reaction mixture

from pale green to reddish brown. However, confirmation of the presence of AgNPs was done by recording Uv visible absorption spectrum in the region of 300 – 700 nm. Size and size distribution of the silver nanoparticle could be estimated by Uv-visible absorption spectroscopy (Paramelle et al., 2014; Desai et al., 2012). AgNPs with a particle size ranging from 35nm to 50nm obtained by reduction with hydrazine hydrate and sodium citrate, show an absorption maximum at around 420 nm (Guzman et al., 2009). Figure 1 shows Uv-visible absorption spectrum of AgNPs solution synthesized from the extract of *P. hydropiper*.

The λ_{max} values for the AgNPs solution is 426 nm. The spectrum recorded in the same wavelength range, for the extract before treating with $AgNO_3$ solution do not show any absorption band, but only a background. The results are indicative of the formation of AgNPs. Full width at half maximum (FWHM) represents the particle size distribution. Repeated recording of the Uv-visible extinction spectrum of the same as prepared dilute AgNP solution with regular intervals of one week did not show any change in the FWHM, position of λ_{max} and the absorption intensity up to 60 days. This observation exhibits the remarkable stability of the particles.

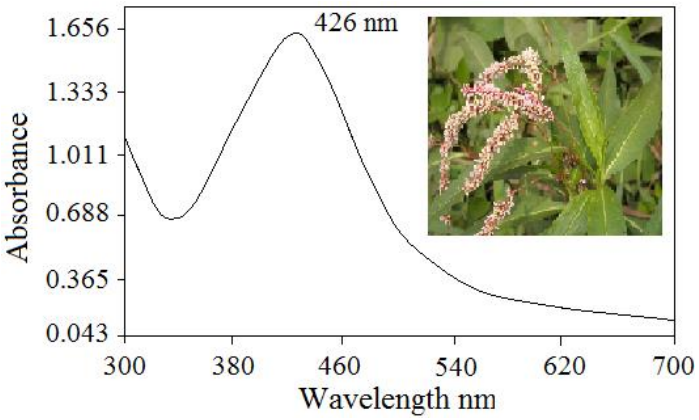

Fig. 1. Uv-visible extinction spectrum of the AgNPs synthesized from the extract of *P. hydropiper*. Inset is the picture of plant with flowers.

Two different sets of experiments were conducted to understand the dependence of the concentration of phytonutrients in the extracts and the concentration of $AgNO_3$, on the particles size of the AgNPs. Uv-visible absorption spectra recorded for the AgNP solutions obtained by reacting 6.0×10^{-5} M $AgNO_3$ with increasing concentrations of the extracts is shown in figure 2. Concentration of the phytonutrients was varied from 4.625×10^{-5} g/mL to 23.125×10^{-5} g/mL.

Absorption maximum is 415 nm when the phytochemicals concentration is 4.625×10^{-5} g/mL (figure 2 (a)). It may be noticed that as the concentration of extract increases, the λ_{max} decreases slightly. The decrease in λ_{max} represents a small reduction in particle size. Therefore an increase in phytonutrient concentration results in a small decrease in particle size.

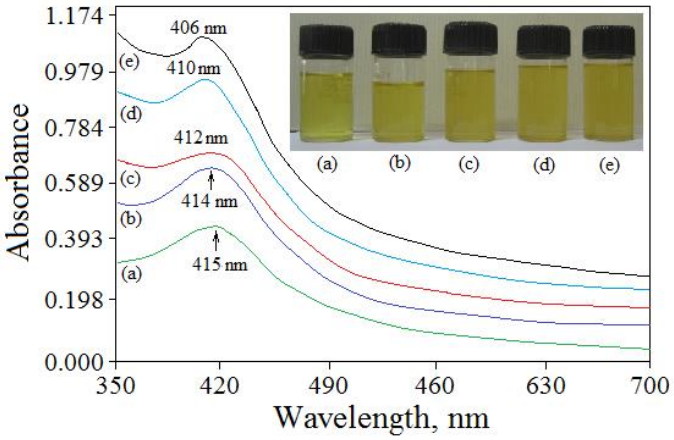

Fig. 2. Uv-visible extinction spectra of the AgNPs synthesized by reaction of 6.0×10^{-5} M $AgNO_3$ with the water extracts of *P. hydropiper* containing (a) 4.625×10^{-5} g/mL, (b) 9.250×10^{-5} g/mL, (c) 13.875×10^{-5} g/mL, (d) 18.50×10^{-5} g/mL and (e) 23.125×10^{-5} g/mL of phytonutrient concentration.

It may also be noticed from figure 2 that the absorption edge at 350 nm raises as the extract concentration increases. The absorption edge towards 300 nm (figure 1) is due to absorption by phytonutrients present in the extract. Therefore, as the extract concentration increases absorption edge at 350 nm increases (figure 2(a) to 2(e)), whereas the absorption intensity or the absorbance, with respect to a baseline between 350 nm and 700 nm remains the same. This observation reflects the fact that, at a fixed concentration of $AgNO_3$, increase in phytonutrient concentration suppresses the particles size to very little extent with no change in the yield of the particles. This may be due to the following reason. As the phytonutrient concentration increases, rate of reduction increases. As soon as particles are formed, since the source of the particles, $AgNO_3$ is limited in the system, capping of the particles preferentially takes place, rather than their growth in to bigger sizes. The inset in figure 2 is the picture of the AgNP solutions corresponding to the Uv-visible extinction spectra, whose same intensity of the colour represents the same concentration of AgNPs with a very small decrease in the particle size from (a) to (e).

Effect of the concentration of $AgNO_3$ at fixed extract concentration on the particle size could be understood from figure 3.

The λ_{max} measured for the AgNP solution obtained by reacting 6.0×10^{-5} M of $AgNO_3$ at a phytonutrient concentration of 9.250×10^{-5} g/mL is 414 nm (figure 3(a)). At the same extract concentration, when the $AgNO_3$ concentration is 0.88×10^{-3} M,

particles with an increase of both λ_{max} as well as absorbance resulted (figure 3(b)).

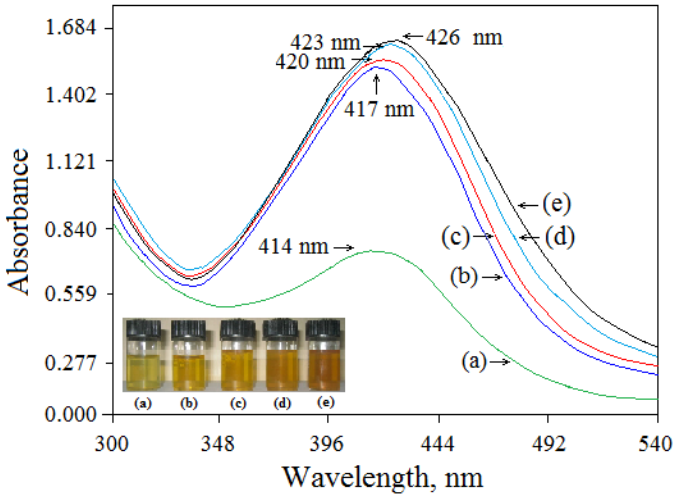

Fig. 3. Uv-visible extinction spectra of the AgNPs synthesized by the reaction of the water extract of *P. hydropiper* containing 9.250×10^{-5} g/mL of phytonutrients in (a) 6.0×10^{-5} M, (b) 0.88×10^{-3} M, (c) 1.76×10^{-3} M, (d) 2.65×10^{-3} M and (e) 3.53×10^{-3} M $AgNO_3$ solution.

The 3 nm increment in λ_{max} may be accounted for by the increase in particle size and the raise in absorbance may be due to a 15 times increase in $AgNO_3$ concentration and the corresponding raise in yield of the particles. Figure 3(b) to figure 3(e) are the Uv-visible extinction spectra recorded for AgNPs prepared by only a two fold increase in concentration of $AgNO_3$ with a fixed 9.250×10^{-5} g/mL of extract concentration. The spectra show a 3 nm increase in λ_{max} from figure 3(b) to figure 3(e) which is an indication of increasing particle size. Therefore, the increment in λ_{max} with raise in $AgNO_3$ concentration may be attributed to increase in the particle size. Thus, particle size of the AgNPs can be increased by increasing the $AgNO_3$ concentration with a sufficient constant concentration of phytonutrients in the extract. Inset in the figure 3 reveals a visual evidence for the change in colour (from figure 3(a) to figure 3(e) corresponding to increase in particle size.

AgNP solution giving its λ_{max} at 426 nm (Fig. 1) was centrifuged at 4000 rpm, to isolate the material for recording SEM and EDS spectra, and XRD patterns. SEM and EDS data recorded to understand the morphology of the AgNPs and their elemental composition respectively are presented in figure 4.

SEM image of the AgNPs isolated by centrifugation at 4000 rpm, indicates that the particles are spherical and appeared to be agglomerated to spherical lumps during centrifugation. Elemental composition of the material reveals 87 % silver and 13 % other material consisting of carbon, nitrogen, oxygen etc. The presence of carbon, nitrogen and oxygen appeared in EDS spectrum are due to phytonutrient molecules that were coated upon the particles in order to stabilize them.

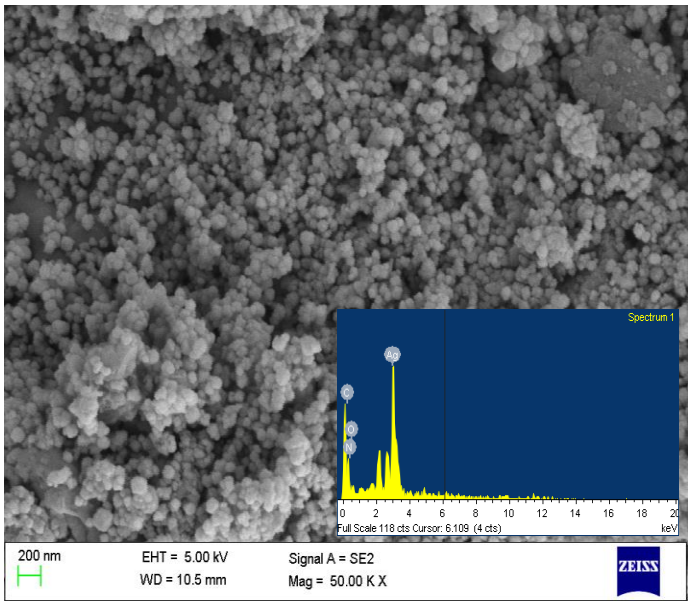

Fig. 4. Scanning electron micrograph of AgNPs synthesized from the leaf extracts of *P. hydropiper*. The inset in the figure shows the EDS spectrum.

Figure 5 shows the TEM image recorded on the drop coated sample of the AgNP solutions.

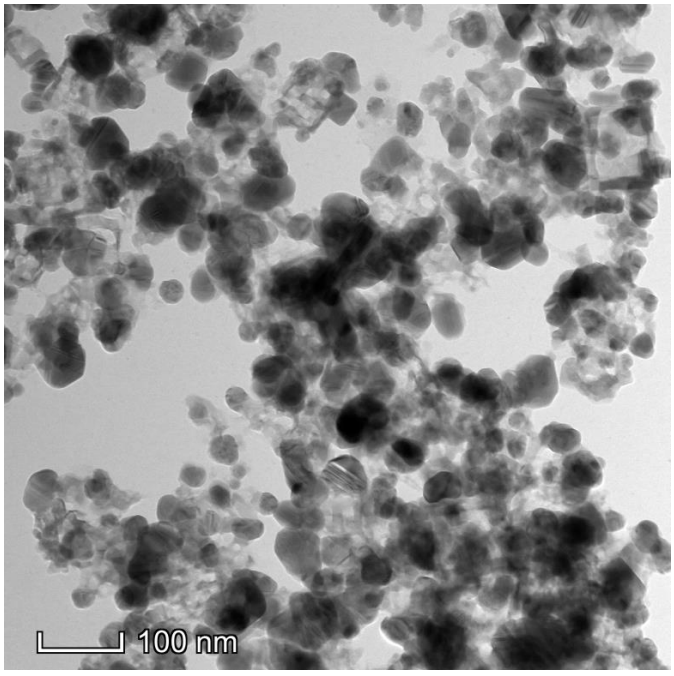

Fig. 5. Transmission electron mocrographs of the AgNPs synthesized from the extracts of *Percicaria hydropiper*.

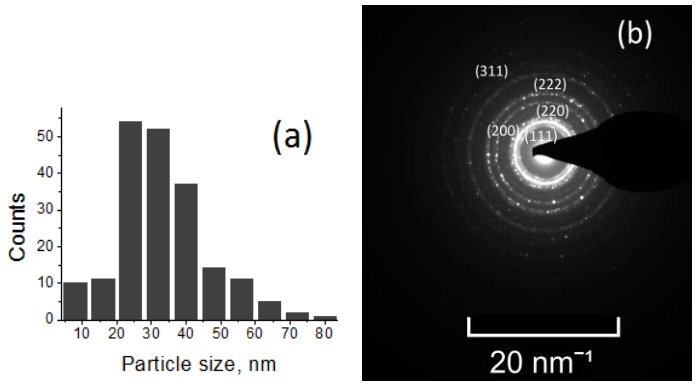

Fig. 6. (a) Particle size distribution of the AgNPs using TEM (Figure 5) and (b) Selected area electron diffraction (SAED) pattern on the AgNPs synthesized from the extract of *P. hydropiper*.

The title AgNPs are spherical and quasi-spherical particles with the higher percentage of the spherical particles. The results are fairly comparable with the TEM studies of the earlier workers and few selective precedents are referenced here. AgNPs prepared using plant, *Terminalia bellirica* extract (Anand & Mandal, 2015) and extracellular synthesis using Fungus, *Aspergillus niger* (Gade et al. 2008) were spherical, and those synthesized using apiin as reducing agent (Kasturi et al., 2009) were quasi-spherical. The particle size distribution histogram, shown in figure 6(a) reveals that particle size distribution has its maximum passing across 24-32 nm. The concentric circles embedded with bright intermittent dots viewed on the selected area electron diffraction (SAED) pattern, shown in figure 6(b), obtained for the AgNP solution, may be ascribed to the 111, 200, 220, 222 and 311 planes of the silver nanparticles crystallized to characteristic face centered cubic (FCC) structure (Guzman et al., 2009). This data is consistent with the reports related to the AgNPs synthesized both by chemical reduction method and by using extract of *Hibiscus rosa sinensis* (Philip, 2010). Particles size estimated in the SEM analysis appears bigger and more uniform compared to that determined by TEM. This may be due to agglomeration of small and big particles having an organic molecular coating, in to bigger lumps of approximately 60-80 nm, during centrifugation and drying in vacuum.

Particle size and crystal structure of the AgNPs is also determined by powder XRD spectrum and the pattern is presented in figure 7.

The crystallographic planes (111), (200), (220), (222), identified in the XRD pattern proves that the reduced metallic silver in the AgNPs synthesized using extract of *P. hydropiper* crystallizes to face centred cubic(FCC) structure.

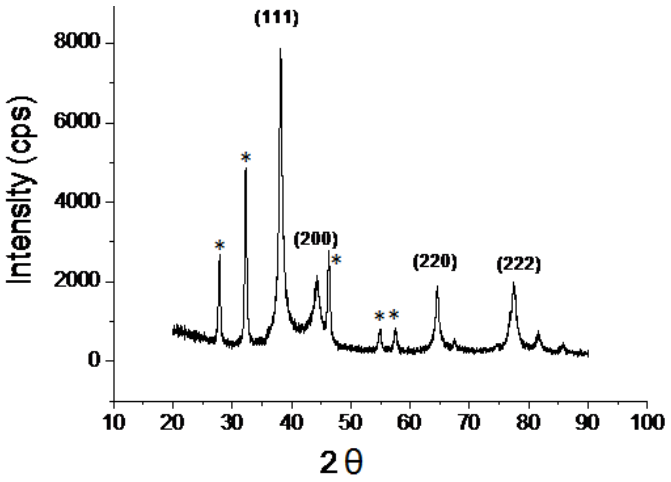

Fig. 7. Powder XRD patterns of AgNPs synthesiszed from extract of *P. hydropiper*.

Relatively higher peak widths of the signals are characteristic of having the metallic silver in nanodimention. Particle size of the AgNPs is calculated using Debye – Scherrer's formula $D = 0.94\ \lambda/\beta \cos\theta$, where D is the average crystalline size, λ is the wavelength of X-ray, β is full width at half maximum and θ is the angle of diffraction. The particle size is worked out to be 24 nm with respect to signal corresponding to (111) crystallographic plane at 2θ value of 38.08. The powder XRD data is comparable and consistent with the silver nanoparticles synthesized from aqueous extract of *Ocimum Sanctum and* quercetin (a flavonoid from the same plant) (Jain & Mehata, 2017), root hair extract of *Phoenix dactylifera* (Oves et al., 2018), extracts of garlic, green tea and turmeric (Selvan et al., 2018), extract of *Sida cordifolia* (Pallela et al., 2018). XRD pattern shows some other set of sharp signals which are marked by asterisk in figure 7. These signals may be ascribed to crystallization of any of the phytonutrients which might have not been involved neither in reduction of $AgNO_3$, nor in molecular capping of the particles.

B. *Antibacterial Activity Studies*

Silver nanoparticles are known very much to exhibit antimicrobial properties (Xiu et al., 2012). The literature reports of their antimicrobial activities were elaborately reviewed (Le Ouay & Stellacci, 2015; Roy et al., 2019).

In the present study, the antibacterial properties were examined against the growth of the *E. coli* and *S. aureus* bacteria using well diffusion method. The zone of inhibition is determined for a period of 20 hours and the results are compared with a standard antibacterial substance ciprofloxacin. Results of the growth

inhibition effects of the AgNPs against *E. coli* and against *S. aureus* are shown in figure 8 and figure 9 respectively.

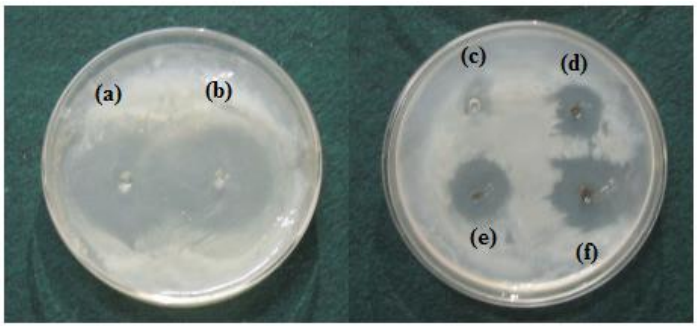

Fig. 8. Growth of *E-coli* bacteria around the scooped holes filled with of (a) 30 µL and (b) 40 µL of ciprofloxacin solution, and (c) 10 µL, (d) 20 µL, (e) 30 µL (f) 40 µL of AgNp solution prepared using water extract of *P. hydropiper*. Concencentration = 60 µg/mL.

AgNP solutions suppress the growth of both the bacteria selected for the study as indicated by a zone of inhibition around the wells (figure 8 and 9). Zone of inhibition to the growth of bacteria is checked in varied volume of the AgNP solutions poured in to the well. Zone of inhibition increases as the quantity of AgNPs increases. Patches (b) in both the figures 8 and 9 are the zones of inhibition to the bacterial growth against 40 microliters of the reference substance and it is measured to be 15.0 mm against both *E. coli* and *S. aureus* bacteria. The zones of inhibition of the AgNPs synthesized using the extract of *P. hydropiper* are 13.0 mm against the growth of *E. coli* (figure 8(f)) and 12.0 mm against the growth *S. aureus* (figure 9(f)).

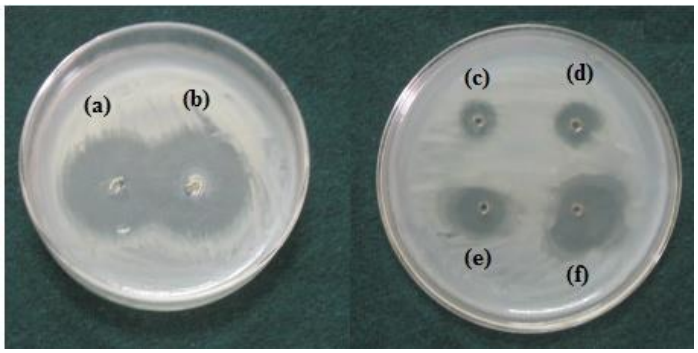

Fig. 9. Growth of *S-aureus* bacteria around the scooped holes filled with of (a) 30 µL and (b) 40 µL of ciprofloxacin solution, and (c) 10 µL, (d) 20 µL, (e) 30 µL (f) 40 µL of AgNp solution prepared using water extract of *P. hydropiper*. Concencentration = 55 µg/mL.

III. CONCLUSION

Silver nanoparticles were prepared using aqueous extract of leaf sample of *P. hydropipr*, a medicinal plant, as reducing agent and stabilizing agent and the particles are very stable. The size of the particles could be controlled by varying the concentrations of $AgNO_3$ and phytonutrients in the extract. The particles were characterized by TEM and PXRD methods to be of an average size of 24 - 32 nm and found to crystallize in to a face cantered cubic structure. The AgNPs exhibits antibacterial activity and inhibit the growth of *E. coli* and *S. aureus* bacteria and data were compared with that of a commercial reference substance, ciprofloxacin. The zones of inhibition were found to be 13.0 mm against *E. coli* and 12.0 mm against *S. aureus*. The antibacterial activity possessed by the title AgNPs is not superior to the reference substance selected, for which the zone of inhibition is 15.0 mm in the same concentration as that of AgNPs.

IV. EXPERIMENTAL SECTION

A. *Materials*

All the chemicals are from Merck, Himedia or from S. D. Fine chemicals. Distilled water was used for all the experiments. R-8C laboratory centrifuge from Remi was used for isolation of particles for SEM and powder XRD analyses. Powder XRD spectra were recorded on a Rigacu Smartlab X-Ray diffractometer and the Scanning electron microscopy (SEM) and energy dispersive x-ray spectroscopy (EDS) were recorded on Ultra 55 scanning electron microscope from GEMINI technology. TEM imaging of the drop coated samples were done on Titan Themis 300kV from FEI. Systronics Uv-visible spectrophotometer 119 was used for recording the Uv-visible extinction spectra in the wavelength range of 300 nm to 700 nm.

B. *Methods*

1) *Extraction*

3 g of the fresh leaves were taken in a mortar and crushed in to paste with a little amount of warm distilled water. The pastes were transferred in to a 250 mL beaker. The contents were added with 100 mL water, stirred on a magnetic stirrer for about 30 minutes at 45-50 °C temperature, cooled to lab temperature and filtered through a piece of ordinary filter paper. 2 mL of the extract was evaporated to dryness on a pre weighed watch glass and then dried in vacuum over anhydrous phosphorous pentoxide in a vacuum desiccator. Weight of the watch galss was taken. Difference in weight of the watch galss before and after evaporation of the extract was 0.0020 g. The well known routine

method was adopted for the qualitative phytochemical analysis of the extracts (Raaman, 2006).

2) Synthesis of Silver Nanoparticles

50 ml of the fresh extract of the selected plant, containing approximately 0.04 ± 0.005 g/mL of extracted substances were taken in a round bottomed flask. Contents were heated to 65 °C while stirring on a magnetic stirrer and 20 mL of 0.002 M $AgNO_3$ solution was added drop wise from a pressure equalizing dropping funnel for exactly 30 minutes. During addition of silver nitrate solution, temperature was maintained at 65 ± 5 °C. Contents were cooled to lab temperature and formation of nanoparticles was confirmed by recording the Uv-visible spectra in the wavelength range of 300 nm to 700 nm. 2 liters of naoparticle solutions were centrifuged for isolation of the AgNPs, for powder XRD and SEM analyses. The samples were then dried in vacuum over anhydrous phosphorous pentoxide.

3) Antibacterial Activity

Well diffusion method was used to determine the antibacterial activity of the AgNPs. To begin with, the amount of AgNPs present in its solution was determined by evaporating know volume AgNP solution on a pre-weighed watch glass, in to complete dryness and taking its weight. The difference in weight will give the amount of AgNPs present per unit volume of its solution. The solution of the standard substance, ciprofloxacin was prepared with the same concentration as that of AgNP solutions. The as prepared AgNPs solutions were used for antibacterial activity studies. The bacteria, cultured in nutrient agar media were obtained from Department of Microbiology, Kuvempu University. The bacteria selected for the study, with their culture accession numbers were *E.coli* (MTCC-1599) and *S. aureus* (MTCC-4734).

Procedure for preparation of nutrient agar media and the antibacterial activity studies may be described as follows. Petri dishes of 8 cm diameter and washed 50 mL beakers and all other required glassware were sterilized in an autoclave. 28 grams of nutrient agar powder was suspended in 1000 mL of distilled water and dissolved by boiling. The contents were autoclaved. 15 mL aliquots of the nutrient agar media were then transferred in to Petri dishes. When the media hardened, the surface of the media was contaminated with bacteria using cotton swabs. The holes are scooped on the media and the holes are filled with different volumes of the AgNP solution and the solution of the reference substance. Petri dishes were incubated at 37 °C for 20 hours. The zones of inhibition were measured.

ACKNOWLEDGEMENT

Author thanks VGST for awarding a K-FIST level-1 grant which was used to establish basic laboratory facility. Author also thank Micro and Nano characterization facility, Center for nanoscience and engineering, IISc., Bangalore for extending characterization support under INUP programme. Author also thanks Dr. B. Thippeswamy, Department of Microbiology, Kuvempu University for giving bacteria.

This research did not receive any specific grant from funding agencies in the public, commercial, or not-for-profit sectors.

REFERENCES

Alex, K. V. et al., (2020) Green synthesized Ag nanoparticles for bio-sensing and photocatalytic applications. *ACS Omega 5*(22), 13123-13129. https://doi.org/10.1021/acsomega.0c01136

Amendola, V., Bakr, O. M., & Stellacci, F. (2010). A study of the surface plasmon resonance of silver nanoparticles by the discrete dipole approximation method: Effect of shape, size, structure, and assembly. *Plasmonics 5*(1), 85-97. DOI: 10.1007/s11468-009-9120-4

Anand, K. K. H., & Mandal, B. K. (2015). Activity study of biogenic spherical silver nanoparticles towards microbes and oxidants. *Spectrochimica Acta A: Molecular and Biomolecular Spectroscopy 135*, 639-645. DOI: 10.1016/j.saa.2014.07.013

Awazu, K.., et al. (2008). A plasmonic photocatalyst consisting of silver nanoparticles embedded in titanium dioxide. *Journal of American Chemical Society 130*(5), 1676-1680. https://doi.org/10.1021/ja076503n

Ayaz, M. et al., (2020). *Persicaria hydropiper* (L.) Delarbre: A review on traditional uses, bioactive chemical constituents and pharmacological and toxicological activities. *Journal of Ethnopharmacology 251*, Article 112516. DOI: 10.1016/j.jep.2019.112516

Baruah, B., Gabriel, G. J., Akbashey M. J., & Booher, M. E. (2013). Facile synthesis of silver nanoparticles stabilized by cationic polynorbornenes and their catalytic activity in 4-nitrophenol reduction. *Langmuir 29*(13), 4225 – 4234. DOI: 10.1021/la305068p

Burdusel, A. C. et al., (2018). Biomedical applications of silver nanoparticles: An up-to-date overview. *Nanomaterials 8*(9), Article 681. DOI: 10.3390/nano8090681

Desai, R., Mankad, V., Gupta, S. K., & Jha, P. K. (2012). Size distribution of silver nanoparticles: UV-visible spectroscopic assessment. *Nanoscience and Nanotechnology Letters* 4(1), 30 – 34. https://doi.org/10.1166/nnl.2012.1278

Gade, A. K. et al., (2008). Exploitation of *Aspergillus niger* for synthesis of silver nanoparticles. *Journal of Biobased Materials and Bioenergy. 2*(3) 243-247.

Garcia, M. A. (2011). Surface plasmons in metallic nanoparticles: Fundamentals and applications. *Journal of Physics D: Applied. Physics 44*(28), Article 283001.

Garcia-Barrasa, J., López-de-Luzuriaga, J. M., & Monge, M. (2011). Silver nanoparticles: Synthesis through chemical methods in solution and biomedical applications. *Central European Journal of Chemistry 9*, 7-19. https://doi.org/10.2478/s11532-010-0124-x

Glavee, G. N., Klabunde, K. J., Sorensen, C. M., & Hadjapanayis. (1992) Borohydride reductions of metal ions. A new understanding of the chemistry leading to nanoscale particles of metals, borides, and metal borates. *Langmuir 8*(3), 771-773. https://doi.org/10.1021/la00039a008

Gopinath, K. et al., (2016). Green synthesis of silver, gold and silver/gold bimetallic nanoparticles using the *Gloriosa superba* leaf extract and their antibacterial and antibiofilm activities. *Microbial Pathogenesis 101*, 1-11. https://doi.org/10.1016/j.micpath.2016.10.011

Guzman, M. G., Dille, J. & Godet, S. (2009). Synthesis of silver nanoparticles by chemical reduction method and their antibacterial activity. *International Journal of Chemical and Biomolecular Engineering 2*(3) 104 – 111.

Jain, P., & Pradeep, T. (2005). Potential of silver nanoparticle-coated polyurethane foam as an antibacterial water filter. *Biotechnology and Bioengineering 90*(1), 59-63. DOI: 10.1002/bit.20368

Jain, S., & Mehata, M. S., (2017). Medicinal plant leaf extract and pure flavonoid mediated green synthesis of silver nanoparticles and their enhanced antibacterial property. *Scientific Reports 7* Article 15867. https://doi.org/10.1038/s41598-017-15724-8

Jensen, T. R., Malinsky, M. D., Haynes, C. L., & Van. Duyne, R. P. (2000). Nanosphere lithography: Tunable localized surface plasmon resonance spectra of silver nanoparticles. *Journal of Physical Chemistry B, 104*(45), 10549 – 10556.

Kasturi, J., Veerapandian, S., & Rajendran, N. (2009). Biological synthesis of silver and gold nanoparticles using Apiin as reducing agent. *Colloids and Surfaces B: Biointerfaces 68*(1), 55-60. DOI: 10.1016/j.colsurfb.2008.09.021

Ko, S. J.et al. (2013). Highly efficient plasmonic organic optoelectronic devices based on a conducting polymer electrode incorporated with silver nanoparticles. *Energy and Environmental Science, 6*(6), 1949-1955. DOI: 10.1039/c3ee40190a

Le Ouay, B., & Stellacci, F. (2015). Antibacterial activity of silver nanoparticles: A surface science insight. *Nanotoday 10*(3), 339 – 354. https://doi.org/10.1016/j.nantod.2015.04.002

Li, W., Guo, Y., and Zhang, P. (2010). SERS-active silver nanoparticles prepared by a simple and green method. *Journal of Physical Chemistry C, 114*(14), 6413–6417. https://doi.org/10.1021/jp100526v

Mandal, D. et al., (2016). Bio-fabricated silver nanoparticles preferentially targets gram positive depending on cell surface charge. *Biomedicine & Pharmacotherapy 83*, 548-558. DOI: 10.1016/j.biopha.2016.07.011

McFarland, A. D., & Van Duyene, R. P. (2003). Single silver nanoparticles as real-time optical sensors with zeptomole sensitivity. *Nano Letters, 3*(8), 1057-1062. https://doi.org/10.1021/nl034372s

Mittal, A. K., Chisti, Y., & Banerjee, U. C. (2013). Synthesis of metallic nanoparticles using plant extracts. *Biotechnology Advances 31*(2), 346 – 356. DOI: 10.1016/j.biotechadv.2013.01.003

Morfa, A. J., & Rowlen, K. L. (2008). Plasmon-enhanced solar energy conversion in organic bulk heterojunction photovoltaics. *Applied Physics Letters, 92*(1), 013504. https://doi.org/10.1063/1.2823578

Moyeenul Huq, A. K. M., Jamal, J. A., & Stanslas, J. (2014). Ethnobotanical, phytochemical, pharmacological, and toxicological aspects of Persicaria hydropiper (L.) Delarbre. *Evidence-Based Complementary and Alternative Medicine 12*, Article 782830, 1-11. DOI: 10.1155/2014/782830

Nogin ov, M. A. et al., (2006). Enhancement of Surface plasmons in an Ag aggregate by optical gain in a dielectric medium. *Optics Letters 31*(20), 3022-3024. https://doi.org/10.1364/OL.31.003022

Oves, M. et al., (2018) Antimicrobial and anticancer activities of silver nanoparticles synthesized from the root hair extract of *Phoenix dactylifera*" *Material Science and Engineering: C 89*, 429-443. DOI: 10.1016/j.msec.2018.03.035

Paramelle, D. et al., (2014). Rapid method to estimate the concentration of citrate capped silver nanoparticles from UV-visible light spectra. *Analyst 139*, 4855-4861. https://doi.org/10.1039/C4AN00978A

Philip D. (2010). Green synthesis of gold and silver nanoparticles using *Hibiscus rosa sinensis. Physica E: Low-Dimensional Systems and Nanostructures 42*(5), 1417 – 1424. DOI: 10.1016/j.physe.2009.11.081

Prabhu, S., & Poulose, E. K. (2012). Silver nanoparticles: Mechanism of antimicrobial action, synthesis, medical applications, and toxicity effects. *International Nano Letters* 2, Article 32. https://doi.org/10.1186/2228-5326-2-32

Priya, R. S., Geetha, D., & Ramesh, P. S. (2016). Antioxidant activity of chemically synthesized AgNPs and biosynthesized Pongamia pinnata leaf extract mediated AgNPs - A comparative study. *Ecotoxicology and Environmental Safety 134*(2), 308 – 318. DOI: 10.1016/j.ecoenv.2015.07.037

Raaman, N. (2006). *Phytochemical Techniques*. New Delhi, India: New India Publishing Agency.

Rai, M., Yadav, A., & Gade, A. (2009) Silver nanoparticles as a new generation of antimicrobials. *Biotechnology Advances 27*(1), 76 – 83. DOI: 10.1016/j.biotechadv.2008.09.002

Rajeshkumar, S., & Bharath, L. V. (2017). Mechanism of plant-mediated synthesis of silver nanoparticles - A review on biomolecules involved, characterisation and antibacterial activity. *Chemico-Biological Interactions 273*, 219 – 227. DOI: 10.1016/j.cbi.2017.06.019

Ravindra, S., Mohan, Y. M., Reddy, N. N., & Raju, K. M. (2010). Fabrication of antibacterial cotton fibres loaded with silver nanoparticles via green approach. *Colloids and Surfaces A: Physicochemical and Engineering Aspects 367*(1-3), 31-40. DOI: 10.1016/j.colsurfa.2010.06.013

Roy, A., Bulut, O., Some, S., Mandal, A. K., & Yilmaz, M. D. (2019) Green synthesis of silver nanoparticles: Biomolecule-nanoparticle organizations targeting antimicrobial activity. *RSC Advances 9*, 2673 – 2702.

Schmid, G., & Chi, L. F. (1998). Metal clusters and colloids. *Advanced Materials 10*(7), 515-526. https://doi.org/10.1002/(SICI)1521-4095(199805)10:7<515::AID-ADMA515>3.0.CO;2-Y

Selvan, D. A., Mahendran, D., Senthil Kumar, R., Rahiman, A. K. (2018). Garlic, green tea and turmeric extracts-mediated green synthesis of silver nanoparticles: Phytochemical, antioxidant and *in vitro* cytotoxicity studies. *Journal of Photochemistry and Photobiology B: Biology 180*, 243 – 252. https://doi.org/10.1016/j.jphotobiol.2018.02.014

Sharma, V. K., Yngard, R. A., & Lin, Y. (2008). Silver nanoparticles: Green synthesis and their antimicrobial activities. *Advances in Colloid and Interface Science 145*(1-2), 83–96. DOI: 10.1016/j.cis.2008.09.002

Song, J., Kang, H., Lee, C., Hwang, S. H., & Jang, J. (2012). Aqueous synthesis of silver nanoparticle embedded cationic polymer nanofibers and their antibacterial activity. *ACS Applied Materials & Interfaces 4*(1), 460-465. https://doi.org/10.1021/am201563t

Stark, W. J., Stoessel, P. R., Wohlleben, W. & Hafner, A. (2015). Industrial applications of nanoparticles. *Chemical Society Reviews 44*, 5793-5905. https://doi.org/10.1039/C4CS00362D

Taleb, A., Petit, C., & Pileni, M. P. (1998). Optical properties of self-sssembled 2D and 3D superlattices of silver nanoparticles. *Journal of Physical Chemistry B 102*(12), 2214-2220. https://doi.org/10.1021/jp972807s

Pallela, P. N. V. K., Ummey, S., Ruddaraju, L. K., Pammi, S. V. N., & Yoon, S.-G. (2018). Ultra small, mono dispersed green synthesized silver nanoparticles using aqueous extract of *Sida cordifolia* plant and investigation of antibacterial activity. *Microbial Pathogenisis 124*, 63-69. https://doi.org/10.1016/j.micpath.2018.08.026

Wong, K. K. Y., & Liu, X. (2010). Silver nanoparticles - The real silver bullet in clinical medicine. *Medicinal Chemistry Communication 1*(2), 125 – 131. https://doi.org/10.1039/C0MD00069H

Wu, M., Ma, B., Pan, T., Chen, S., & Sun, J. (2016). Silver-nanoparticle-colored cotton fabrics with tunable colors and durable antibacterial and self-healing superhydrophobic properties. *Advanced Functional Materials 26*(4), 569-576. https://doi.org/10.1002/adfm.201504197

Xiu, Z. M., Zhang, Q. B., Puppala, H. L., Colvin, V. L., & Alvarez, P. J. J. (2012). Negligible particle-specific antibacterial activity of silver nanoparticles. *Nano Letters 12*(8), 4271−4275. DOI: 10.1021/nl301934w

Yoon, K. Y., Byeon, J. H., Park, C. W., & Hwang, J. (2008). Antimicrobial effect of silver particles on bacterial contamination of activated carbon fibers. *Environmental Science & Technology 42*(4), 1251 – 1255. https://doi.org/10.1021/es0720199

Zhang, S., Tang, Y., & Vlahovic, B. (2016) A review on preparation and applications of silver-containing nanofibers. *Nanoscale Research Letters 11*, Article 80. https://doi.org/10.1186/s11671-016-1286-z

***